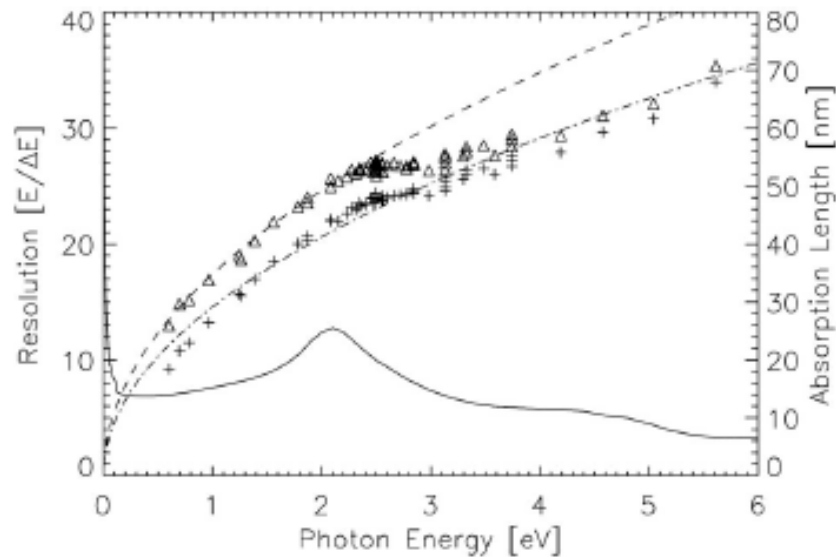

Down-conversion phonon noise in optical TESs

Resolving power of Ta/Al STJ detector



$$R = \frac{E}{2.355\sqrt{1.7\Delta[F + G(\tau)]E}}$$

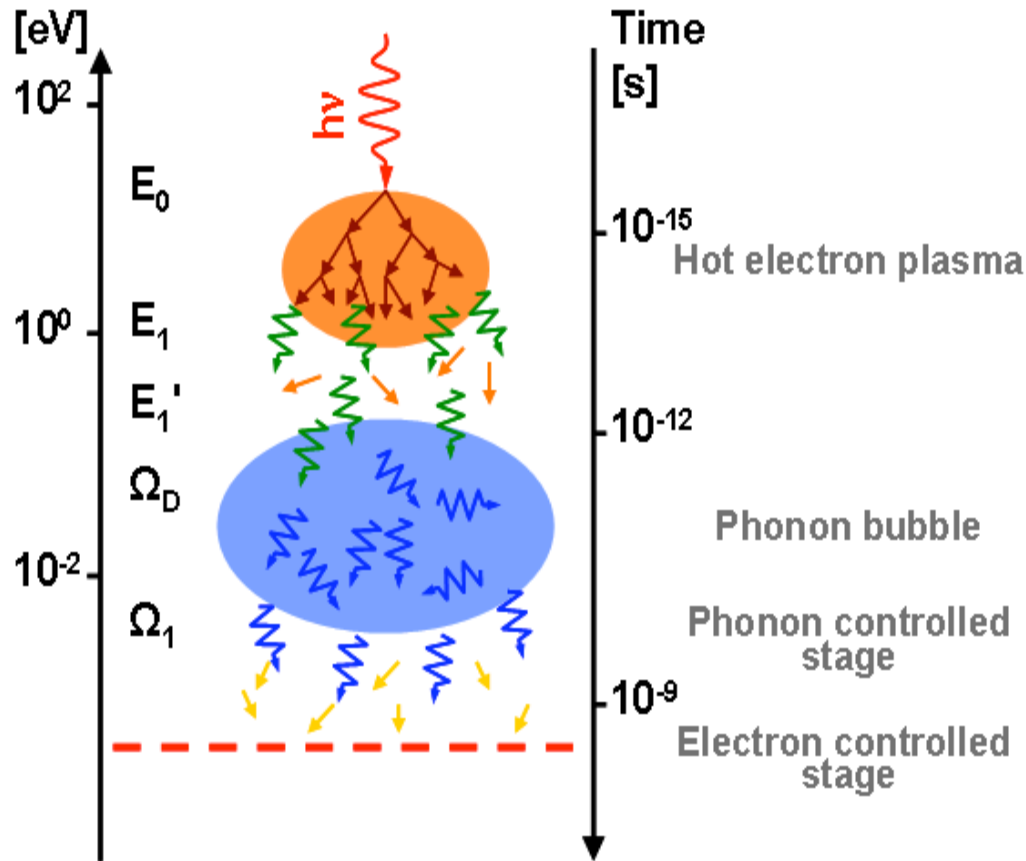
FIG. 1. Energy resolution as function of photon energy (left vertical scale). Crosses are resolution measurements; triangles are the intrinsic resolution calculated from measurements. Drawn curves are the theoretical predictions using Eq. (1) with $F+G=0.7$ (dashed curve) and $F+G=1$ (dotted-dashed curve). The continuous curve is the absorption depth for optical photons in tantalum (right vertical scale).

APL (2006)

Down-conversion phonon noise in TES

- DC: scenario, phonon generation
- Phonon distribution evolution over the spectrum
- Phonon spatial distribution
- Phonon transport properties
- Energy transfer across the escape interface
- Energy loss
- Fluctuations

Electron-phonon down-conversion. Scenario



$$\tau_{e-e}^{-1}(E_1) = \tau_{e-ph}^{-1}(E_1)$$

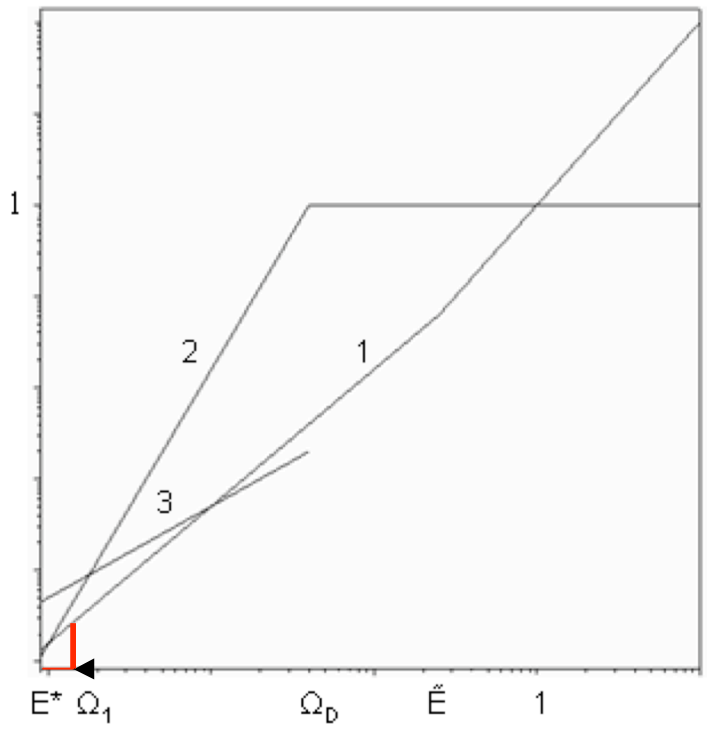
$$\tau_{ee}(E_1') = \frac{E_1'}{2\Omega_D} \tau_s$$

$$\tau_{e-ph}^{-1}(\epsilon) = \tau_s^{-1}(\epsilon/\Omega_D)^3$$

$$E_1' = 2^{\frac{1}{3}} E_1^{\frac{2}{3}} \Omega_D^{\frac{1}{3}} \simeq \Omega_D \left(\frac{E_1}{\Omega_D} \right)^{\frac{2}{3}} \gg \Omega_D$$

$$\Omega_1 = \Omega_D (\tau_s / \tau_{ph-e}(\Omega_D))^{1/2}$$

Electron-phonon down-conversion in TES



Characteristic time scales:

$$\tau_s \approx 10 \div 100 \text{ fs}, \quad \tau_{ph-e}(\Omega_D) \approx 1 \div 10 \text{ ps}$$

Characteristic energies:

$$E^* \leq \Omega_1 \approx 1/10 \Omega_D \ll \Omega_D \approx 1/20 \div 1/30 E_1 \ll \tilde{E} \leq E_1$$

Schematic dependence of electron-electron, electron-phonon and phonon-electron interaction rates as a function of energy. Energy in units of E_1 . $\tau_s \tau_{e-e}^{-1}(\epsilon)$ - curve 1; $\tau_s \tau_{e-ph}^{-1}(\epsilon)$ - curve 2; $\tau_s \tau_{ph-e}^{-1}(\epsilon)$ - curve 3;

Electron-phonon down-conversion stage

$E_1 \rightarrow \Omega_D$: phonon bubble

$$\frac{\partial n}{\partial t} - D\Delta n = I_{ep}\{n\} + I_{ee}\{n\} + Q(\epsilon, \mathbf{x}, \mathbf{x}_0, t)$$
$$\frac{\partial N}{\partial t} = I_d\{N\} + I_{pe}\{N\}$$

Here $n = n(\epsilon, \mathbf{x}, t)$ and $N = N(\Omega, \mathbf{x}, t)$ are distribution functions for qps and phonons, respectively, depending on qp energy, ϵ , phonon energy, Ω , position \mathbf{x} , and time t , D is the qp diffusion coefficient, $I_{ee}\{n\}$, $I_{ep}\{n\}$, $I_d\{N\}$, and $I_{pe}\{N\}$ are the collision integrals describing, respectively, electron-electron (e-e) collisions, collisions between qps and phonons, phonon loss into the substrate, and collisions between phonons and qps. Q is the source term, depending also on the position of the absorption site \mathbf{x}_0 .

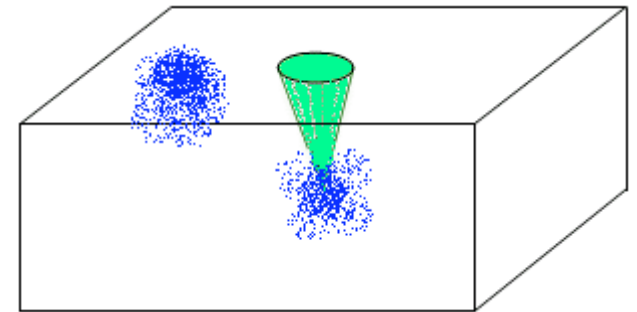
Electron-phonon down-conversion stage

$E_1 \rightarrow \Omega_D$: phonon bubble

$$\frac{\partial n}{\partial t} - D\Delta n - \frac{\lambda\Omega_D}{4}\hbar\Omega_D\frac{\partial n}{\partial \epsilon} = Q \quad \longrightarrow \quad n(\mathbf{x}, t) = \frac{1}{2d\pi Dt} \sum_{m=0}^{\infty} \frac{1}{1 + \delta_{m,0}} \cos \left[m\pi \left(\frac{1}{2} + \frac{z}{d} \right) \right] \cos \left[m\pi \left(\frac{1}{2} + \frac{z_0}{d} \right) \right] \exp \left(-\frac{m^2\pi^2 Dt}{d^2} - \frac{(\mathbf{r} - \mathbf{r}_0)^2}{4Dt} \right)$$

phonon distribution in the bubble

$$\tilde{N}(\Omega, z, z_0, t_{dc}) = \frac{1}{A} \frac{E}{\Omega_D} \frac{8}{\beta\Omega_D^3 d} \sum_{m=0}^{\infty} \frac{\kappa(m^2\zeta^2)}{1 + \delta_{m,0}} \cos \left[m\pi \left(\frac{1}{2} + \frac{z}{d} \right) \right] \cos \left[m\pi \left(\frac{1}{2} + \frac{z_0}{d} \right) \right]$$



$$\kappa(x) = \exp(-x) \sinh(x)/x, \quad \zeta^2 = \pi^2 Dt_{dc}/2d^2$$

$$t_{dc} = \frac{4}{3}\tau_s \left(\frac{E_1}{E'_1} \right)^2 = \frac{1}{3} \left(\frac{4E_1}{\Omega_D} \right)^{\frac{2}{3}} \tau_s$$

t_{dc} is the duration of $E_1 \rightarrow \Omega_D$ stage

$E_1 \rightarrow \Omega_D$: Energy loss

$$E_{loss}^{\pm} = A \int_0^{\infty} dt \mathbf{q} \left(\pm \frac{d}{2}, t \right) \cdot \mathbf{n} \left(\pm \frac{d}{2} \right)$$

$$E_{loss}(z_0) = E_{loss}^+ + E_{loss}^- = 4E \sum_{m=0}^{\infty} \frac{\kappa(m^2 \zeta^2) \cos m\pi (1/2 + z_0/d)}{1 + \delta_{m,0}}$$

$$\int_0^1 d\xi \xi \eta(m, \xi) \int_0^{\Omega_D} \frac{d\epsilon}{\Omega_D} \left(\frac{\epsilon}{\Omega_D} \right)^3 \frac{l_{pb}(\epsilon)}{d} \frac{[1 - \exp(im\pi - d/l_{pb}(\epsilon)\xi)]}{1 + m^2 \pi^2 l_{pb}^2(\epsilon) \xi^2 / d^2}$$

$$P_s(z, E) = \frac{\exp[-((-1)^s z + d/2)/L(E)]}{L(E)[1 - \exp(-d/L(E))]}$$

$$E_{loss}^s = 4E \sum_{m=0}^{\infty} \frac{\kappa(m^2 \zeta^2)}{1 + \delta_{m,0}} \frac{(-1)^{ms} [1 - \exp(im\pi - d/L(E))]}{[1 - \exp(-d/L(E))][1 + m^2 \pi^2 L^2(E)/d^2]}$$

$$\int_0^1 d\xi \xi \eta(m, \xi) \int_0^{\Omega_D} \frac{d\epsilon}{\Omega_D} \left(\frac{\epsilon}{\Omega_D} \right)^3 \frac{l_{pb}(\epsilon)}{d} \frac{1 - \exp(im\pi - d/l_{pb}(\epsilon)\xi)}{1 + m^2 \pi^2 l_{pb}^2(\epsilon) \xi^2 / d^2}$$

$E_1 \rightarrow \Omega_D$: Energy loss fluctuations

$$\overline{(\delta dM_{\epsilon}^{\pm})^2} = \overline{(\delta dM_{\epsilon}^{\pm})^2}|_e + \overline{(\delta dM_{\epsilon}^{\pm})^2}|_i + \overline{(\delta dM_{\epsilon}^{\pm})^2}|_t$$

angular

interaction

transmission

$$\overline{(\delta E_{loss}^{s,\pm})^2} = \frac{1}{2} \int_{-d/2}^{d/2} dz_0 P_s(z_0, E) \int_{-d/2}^{d/2} dz \int_0^{\Omega_D} d\epsilon \beta \epsilon^4 d\epsilon \int_{\xi_c^{\pm}}^1 d\xi \eta_{\pm}(\xi) \left[(3 - p_{\pm} - \eta_{\pm}(\xi) - \exp\left(-\frac{d/2 \mp z}{l_{pb}(\epsilon)\xi}\right)) \right]$$

$$\tilde{N}(\epsilon, \xi, z, z_0, t_{dc}) \exp\left(-\frac{d/2 \mp z}{l_{pb}(\epsilon)\xi}\right)$$

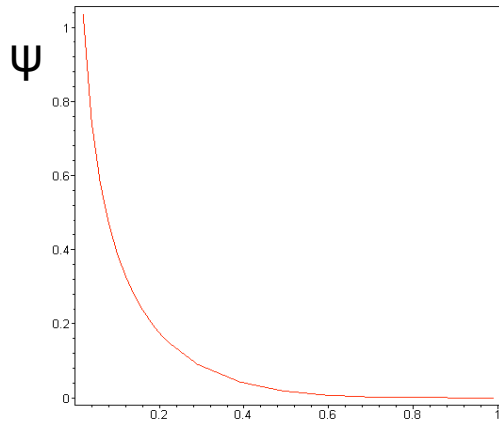
$$\overline{(\delta E_{loss}^s)^2} = (J_+^s + J_-^s) \epsilon E$$

$$J_{\pm}^s = \frac{4\Omega_D}{\epsilon} \sum_{m=0}^{\infty} \frac{\kappa(m^2 \zeta^2)}{(1 + \delta_{m,0})} \frac{(-1)^{m[s+(1\pm 1)/2]} [1 - \exp(im\pi - d/L(E))]}{[1 - \exp(-d/L(E))] [1 + m^2 \pi^2 L^2(E)/d^2]} \int_0^{\Omega_D} d\left(\frac{\epsilon}{\Omega_D}\right) \left(\frac{\epsilon}{\Omega_D}\right)^4 \frac{l_{pb}(\epsilon)}{d} \int_{\xi_c^{\pm}}^1 d\xi \xi \eta_{\pm}(\xi) \left[(3 - p_{\pm} - \eta_{\pm}(\xi)) \frac{1 - \exp[im\pi - d/l_{pb}(\epsilon)\xi]}{1 + m^2 \pi^2 l_{pb}^2(\epsilon) \xi^2 / d^2} - \frac{2[1 - \exp[im\pi - 2d/l_{pb}(\epsilon)\xi]]}{4 + m^2 \pi^2 l_{pb}^2(\epsilon) \xi^2 / d^2} \right]$$

$$J^s(E) = J_1^s(E) + J_2^s(E) + \dots \quad ? \Omega_D \rightarrow \Omega_1 ? \quad E_{loss}^s = (a_+ J_+^s + a_- J_-^s) \frac{\epsilon}{\Omega_D} E$$

$\Omega_D \rightarrow \Omega_1$: Energy loss fluctuations

$$J_{\Omega_D \rightarrow \Omega_1}^{\pm} = \frac{12}{17} p_{\pm} \frac{1 + \zeta_c^{\pm}}{2} \frac{\Omega_D}{\epsilon_0} \frac{l_{pbD}}{d} \Psi \left(\frac{\Omega_1}{\Omega_D} \right)$$



Graph of ψ as a function of Ω_1/Ω_D :
 $\eta=0.76$, $p=0.07$.

For Al/Al₂O₃ interface $\Omega_1/\Omega_D=0.09$
 $\psi=0.43$

$$J_{\Omega_D \rightarrow \Omega_1}^{\pm} = 0.23$$

Ω_1/Ω_D

$$\frac{\partial \tilde{N}}{\partial t} + c \nabla \tilde{N} + \lambda_1 \epsilon \tilde{N} = Q$$

$$Q = 2\lambda_1 \int_{\epsilon}^{\infty} d\epsilon' N(\epsilon', \mathbf{x}, t)$$

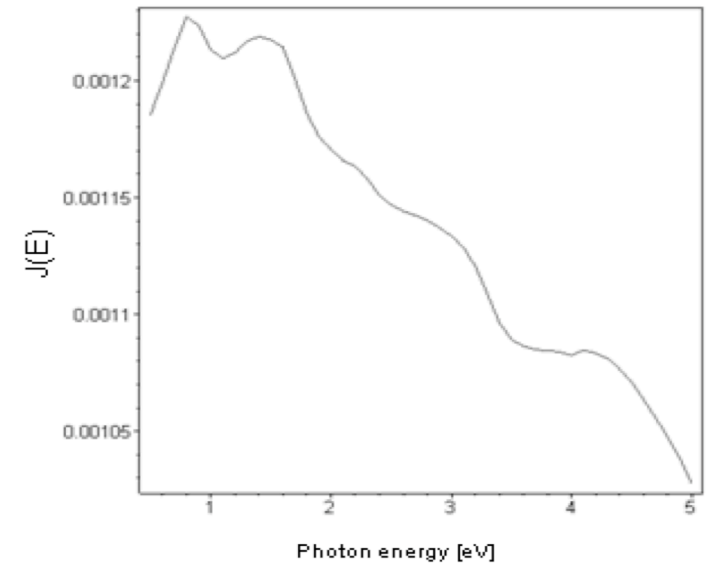
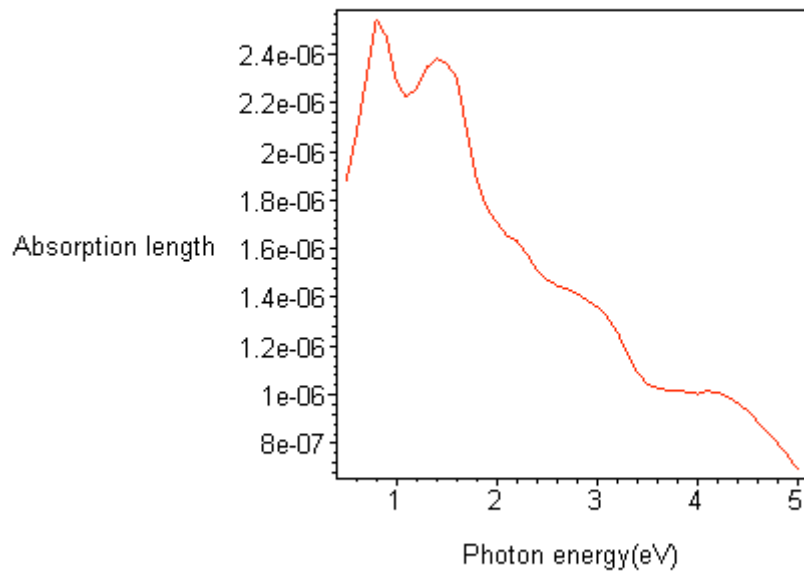
$$\left\{ \left(\frac{\epsilon'}{\epsilon} \right)^3 - \text{Re} \left[\left(1 - \frac{5i\sqrt{2}}{4} \right) \left(\frac{\epsilon'}{\epsilon} \right)^{-i\sqrt{2}} \right] \right\} \Theta(\xi - \xi_c)$$

$$N(\epsilon', \mathbf{x}, t) = \frac{22}{17} \frac{E}{\beta V_{TES} \epsilon^3} \frac{\lambda_1 t \Theta(\epsilon - \Omega_1) \Theta(1 - \lambda_1 \epsilon t)}{1 - \lambda_1 \Omega_1 t}$$

Down-conversion noise in TESs. W

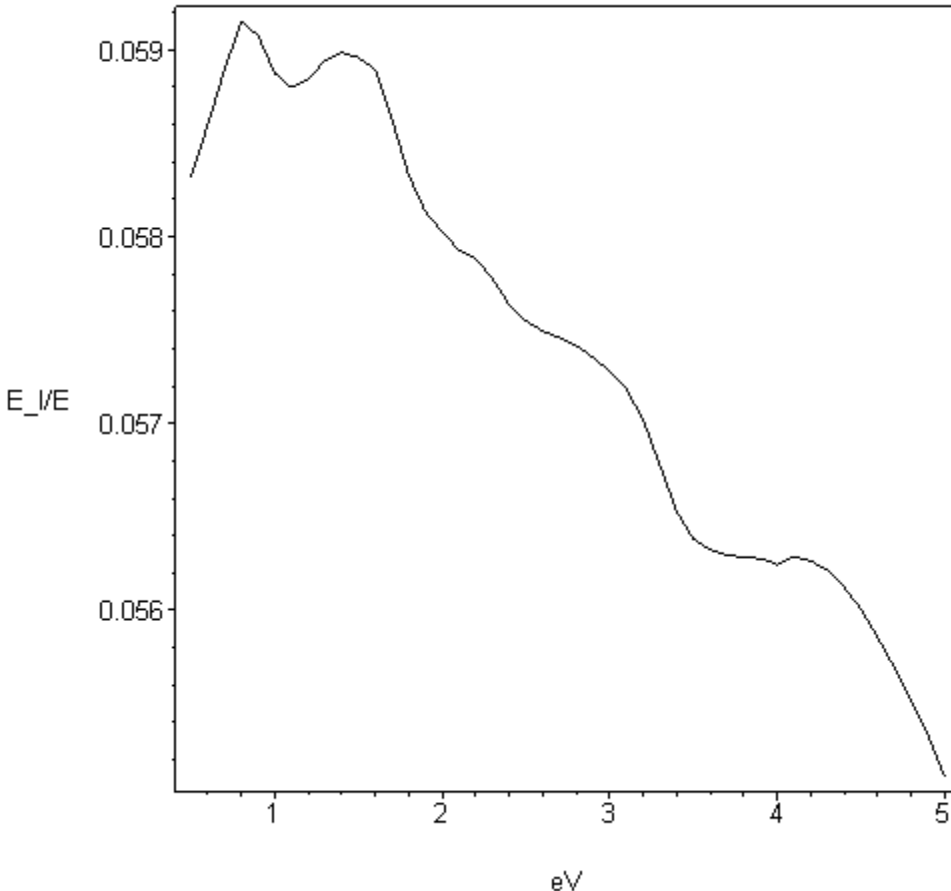
$$\Delta E = 2.355 \sqrt{4k_B T_c \sqrt{n/2} E_{max} / \kappa^2 + JE}$$

Absorption length as a function of photon energy in W



Down-conversion noise in TESs. W

Energy loss from W TES during down-conversion



Whilst noise contribution is small (<15%) the energy loss during this stage is significant (~50%)

This is expected, because phonons of lower energy generations possess longer mean free paths and all reach escape interface. At the same time their numbers increase leading to a decrease of fluctuations

Down-conversion noise in TESs. W

$$\Delta E = 2.355\sqrt{4k_B T_c \sqrt{n/2} E_{max} / \kappa^2 + JE}$$

Energy resolution of W TES in optical range

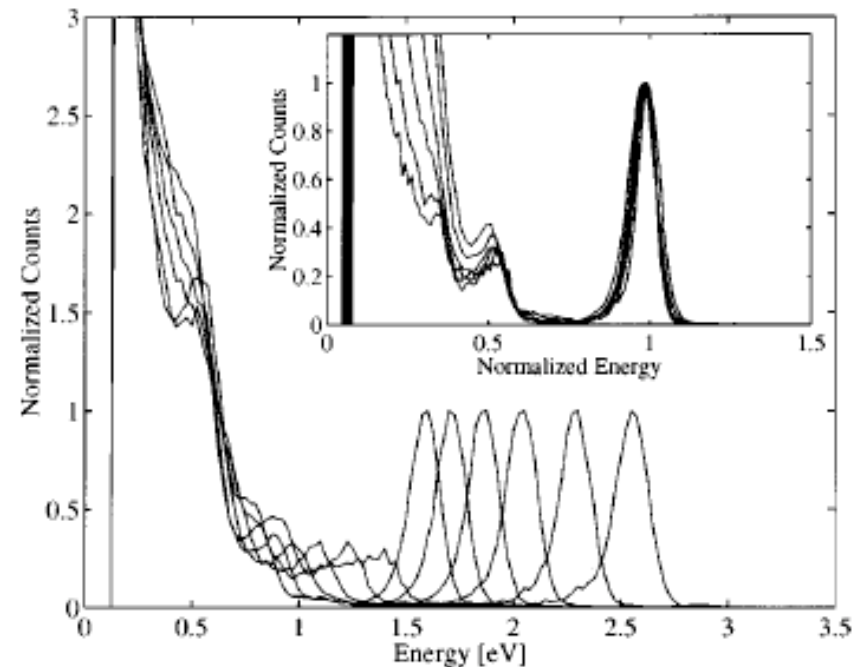
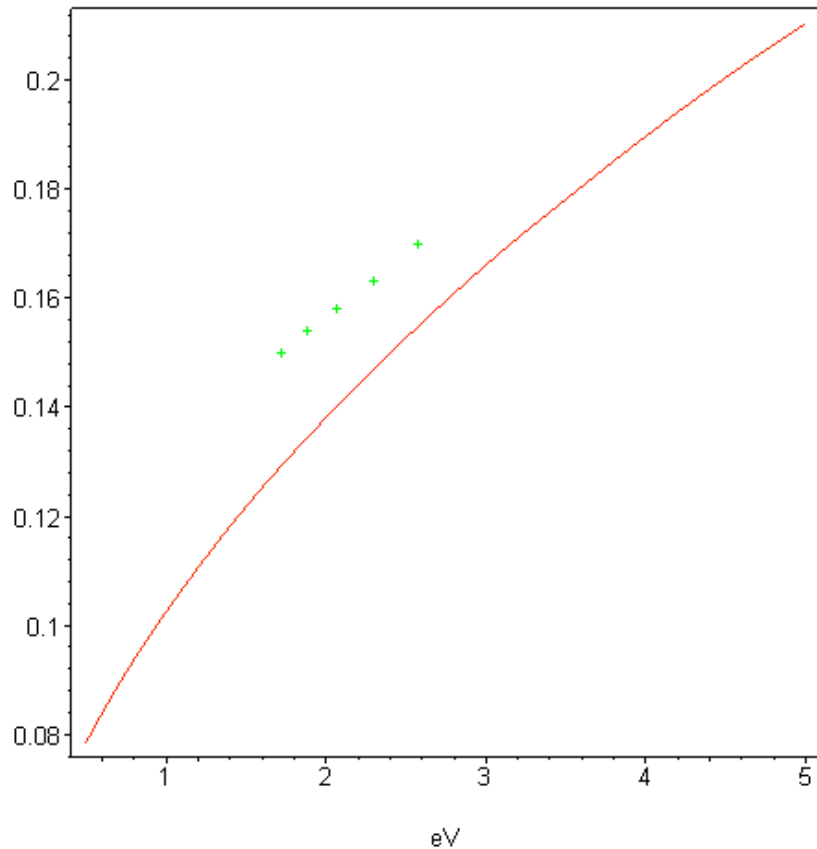
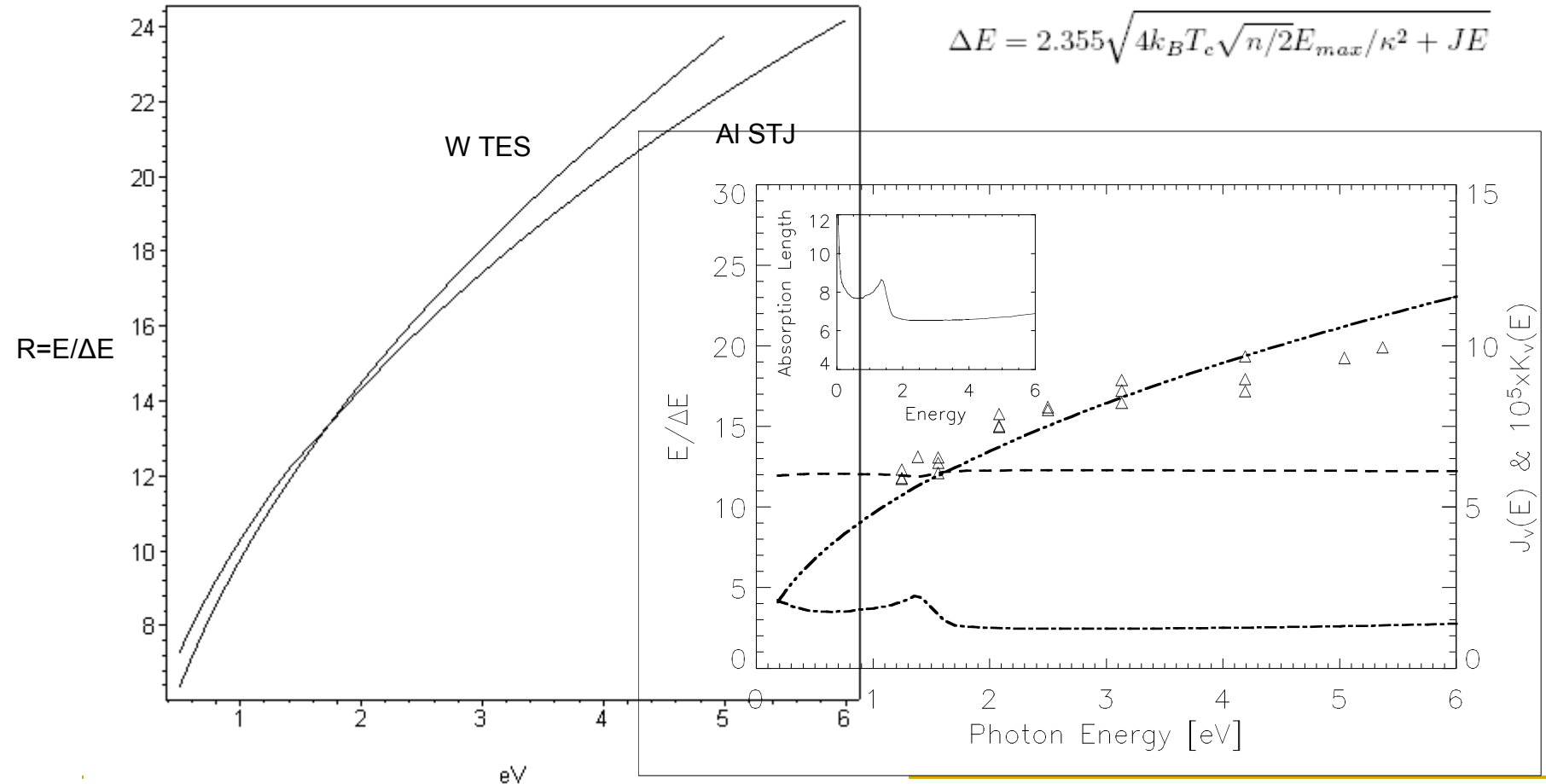


FIG. 3. Pulse height spectra using incident photons from a monochromator at 480, 540, 600, 660, 720, and 780 nm. The counts have been normalized to the same peak height and show a low energy feature below 0.6 eV ($2 \mu\text{m}$) due to IR emission, and features near half the peak energy (see inset with normalized energy) due to photons which hit the rails.

Down-conversion noise in Al STJ and W TES in optical range. Comparison

Resolving power of Al STJ and W TES

$$\Delta E = 2.355 \sqrt{4k_B T_c \sqrt{n/2} E_{max} / \kappa^2 + JE}$$



Down-conversion noise in Ta/Al STJ and W TES in optical range. Comparison

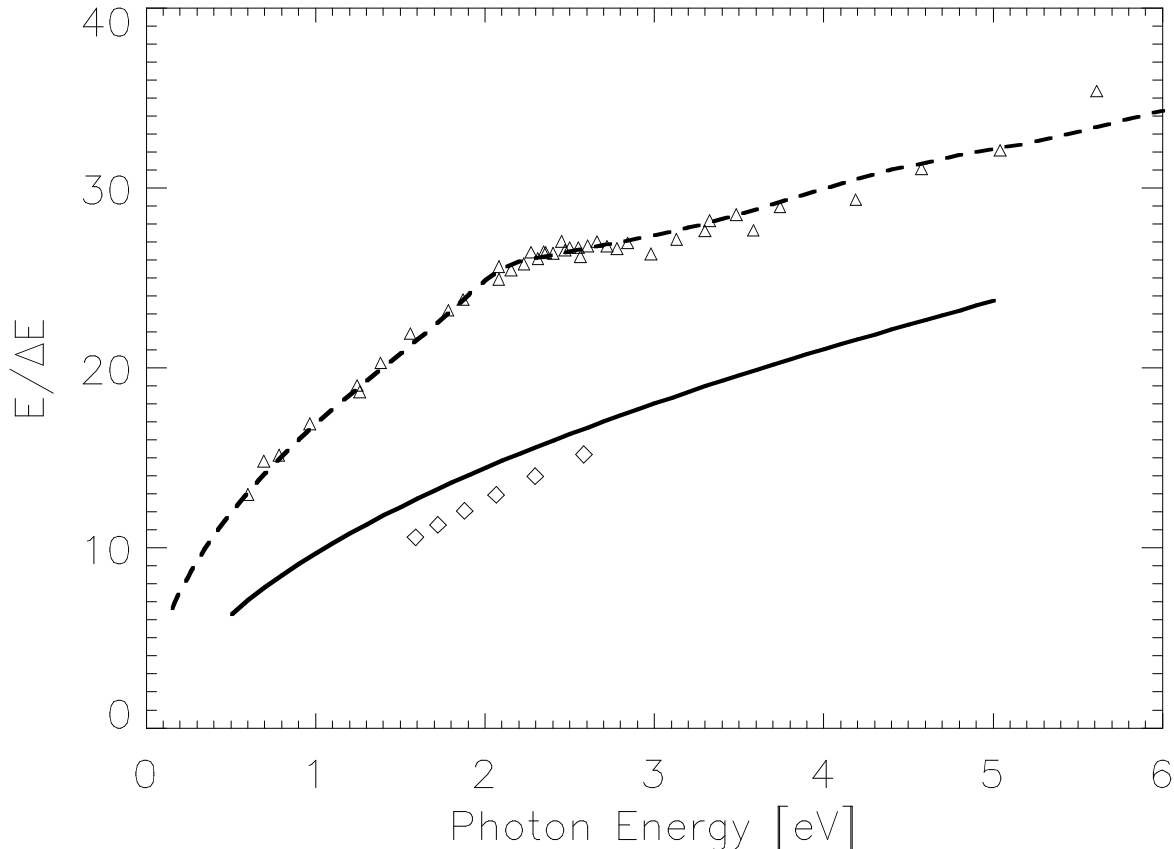


FIG. 3: Resolving power as a function of photon energy: upper curve and experimental points - Ta/Al STJ⁴, lower curve - calculated result for TES detector, points - data from²

Ref.4 – D.Martin *et al*
APL, **88** 123510 (2006)
Ref.2 – B.Cabrera *et al*
APL, **73**, 735 (1998)

Summary

In summary, we have proposed the existence of an important, additional source of noise in TES photon detectors, and presented evidence that it is the main limitation of resolving power in the optical regime.